JOURNAL OF MATERIALS SCIENCE 27 (1992) 2243–2250

Influence of an external electric field on the microstructure of superplastically deformed 7475 Al

XIAO-PING LU, WEI-DI CAO, A. F. SPRECHER, H. CONRAD
Department of Materials Science and Engineering, North Carolina State University, Raleigh, NC 27695-7907, USA

An externally applied electric field retarded strain-enhanced grain growth and promoted dynamic recrystallization during superplastic deformation of 7475 Al. Also, a more extensive dispersoid-free zone was observed in specimens deformed in the electric field, suggesting that the electric field increased the contribution of diffusion creep to superplastic deformation. The electric field promoted the coarsening of dispersoids, especially in the vicinity of the grain boundaries. Possible mechanisms for the observed effects are discussed.

1. Introduction

Previous studies have shown that microstructural instability accompanies superplastic deformation of metals [1–3]. In a precipitation hardening alloy such as 7475 Al, this can include strain-enhanced grain growth, dissolution and/or coalescence of precipitate and dispersoid particles and formation of dispersoid-free zones (DFZ). Such microstructural instability is of interest because it has an influence on the superplastic deformation behaviour and on the resultant microstructure which governs the subsequent mechanical properties. The strain-enhanced grain growth causes "hardening" in the sense that it increases the flow stress for a given strain rate [4], reduces the failure strain [5, 6] and promotes cavitation [7, 8]. The dissolution/precipitation reaction and DFZ formation can significantly change the plastic flow behaviour and also affect cavitation during superplastic deformation [9]. One possible reason for the effects of the dissolution/precipitation and DFZ formation on plastic flow and cavitation is through their influence on strain-enhanced grain growth. In addition, DFZ formation may be related to the contribution of diffusion creep to superplastic deformation [10, 11].

Microstructural instability, especially strain-enhanced grain growth, has been investigated in superplastic alloys as a function of temperature, plastic strain and strain rate [12, 13]. Moreover, our previous investigations [14–17] have shown that an external electric field can also have a significant influence on superplastic deformation and cavitation of the 7475 Al alloy: an electric field reduced the flow stress and strain-hardening rate (or accelerated strain softening) and significantly suppressed cavitation. These effects are no doubt closely associated with the changes in microstructure which occur during superplastic flow in the presence of an electric field. Therefore, the objective of the present work was to examine the microstructural variations which occur during superplastic flow of 7475 Al in an external electric field, with the goal of obtaining a better understanding of the influence of an electric field on superplastic deformation.

2. Experimental procedure

2.1. Materials

The 7475 Al alloy used in this study was provided by Alcoa Research Laboratories (Alcoa, PA); its nominal chemical composition is given in Table I. The as-received, ~ 1.2-mm-thick sheet was in the recrystallization-annealed condition, a thermomechanical treatment having been used to produce the fine three-dimensional grain structure shown in [15]. The grains are nearly equiaxial, with an aspect ratio less than two at any orientation, but are finer near the sheet surface than at the centre. The mean linear intercept grain sizes on the TS, LS and LT cross sections (L is the longitudinal (length); T is the transverse (width) and S is the short (thickness) are included in Table I.

2.2. Superplastic deformation test

Tensile specimens (7-mm gauge length, 4 mm wide and original sheet thickness) were machined parallel to the rolling, L, direction from the as-received sheet. The tensile tests were conducted at constant temperature (516 °C) and constant elongation rate (crosshead speed of 0.05 cm min^{-1}, corresponding to an initial strain rate of 1.2×10^{-3} s^{-1}). The test specimen was held in the furnace by ceramic grips, and two parallel stainless steel electrode plates were located at a spacing of 10 mm from the sides of specimen in the manner shown in [15, 17]. When the electric field was applied, the specimen was connected to the positive terminal of a commercial high voltage d.c. power supply and the electrodes to the negative terminal. A voltage of 2 kV, corresponding to an electric field of 2 kV cm^{-1}, was applied across the specimen and the electrodes. The specimens were heated at a rate of 20 °C min^{-1} to the

TABLE I Chemical composition and grain size of the 7475 Al alloy

Alloy	Nominal chemical composition (wt %)								Grain size (mm)		
	Cu	Mg	Zn	Mn	Cr	Ti	Si	Fe	TS	LS	LT*
I	1.2 to 1.9	1.9 to 2.6	5.2 to 6.2	0.6 max.	0.18 to 0.25	0.06 max.	0.1 max.	0.12 max.	8.6	9.4	9.6

* Grain size on section parallel to the sheet surface.

test temperature and held there for about 20 min prior to testing. The electric field was first applied at the start of the deformation.

2.3. Microstructure observations

The tensile tests were interrupted at the selected engineering strains of 50, 100 and 150%, and maximum elongation. Two microstructural states were then created by varying the post-deformation heating and cooling conditions.

2.3.1. Deformed state

Normally, the deformed specimens were cooled without an electric field from the test temperature to ambient temperature at a rate of $\sim 15\,^{\circ}C\,s^{-1}$. However this rate was too slow to stop the precipitation reaction during cooling. Therefore a post-deformation heat treatment was performed on the deformed and cooled specimens, which consisted of reheating the specimens to 483 °C for 3–5 s without an electric field, and then quenching into water. This treatment dissolved almost all of the precipitates formed during the prior cooling, and presumably gave a microstructure similar to that existing at the deformation temperature. This microstructural state is termed the deformed state in the discussion to follow.

2.3.2. Precipitated state

This state was obtained on cooling the deformed specimens at the rate of $\sim 15\,^{\circ}C\,s^{-1}$ without the electric field. Extensive precipitation now occurred during cooling, and this state of microstructure is termed the precipitated state.

The following microstructure observations were performed.

2.3.3. Grain growth

The deformed state specimens, together with undeformed reference specimens (taken from the grip region of the deformed state test specimen and therefore subjected to the same time, temperature and electric field), were metallographically polished using standard procedures and etched to reveal grain boundaries by immersing for 10–30 s in Keller's reagent (10 ml HNO_3 + 1.5 ml HCl + 1 ml HF + 87.5 ml H_2O). The mean linear intercept grain size in the specimens deformed to the various strain levels (including the undeformed grip section) was measured on the LT section (after grinding and polishing approximately midway through the sheet thickness) by optical microscopy, and the strain dependence of grain growth established.

2.3.4. Dispersoid-free zone

The DFZ in specimens deformed without and with electric field and in the different post-deformation heating and cooling conditions was examined by optical and transmission electron microscopy (TEM) to determine the dislocation structure, state of second phase particles (precipitates and dispersoids) and geometric parameters of the DFZ. The TEM observations were only performed on the specimen with 100% elongation. For these, 3-mm disks were cut from the gauge length of specimens in the deformed and the precipitated states, and mechanically ground to a thickness of 60–80 μm. They were then chemically thinned to a thickness of 30–40 μm, and finally electrolytically thinned to perforation in a twin-jet electropolisher using a 25% nitric acid–methanol solution. For the optical microscope observations, the DFZ was clearly revealed by immersing metallographically polished specimens in the precipitated state for 5–10 s in a 10% NaOH solution at 70 °C. The mean linear DFZ width, $\bar{S}$, in the direction of extension and the mean DFZ spacing, $\bar{L}$, in the same direction were then measured as a function of electric field and plastic strain.

2.3.5. Grain interior

The morphology of dispersoids and precipitates, and the dislocation structure in the interior of the grains, in both the deformed and precipitated states were examined by TEM using the same preparation procedure as above. The aims of these observations were (i) to check if there is any influence of electric field on the morphology of the dispersoids in the deformed state and of the precipitates in the precipitated state; and (ii) to determine if there is any dislocation activity during superplastic flow, and what effect the electric field had on the dislocation structure.

3. Results

3.1. Grain growth

In general, the grain structure of the 7475 Al alloys is relatively stable, and only a small change in grain size

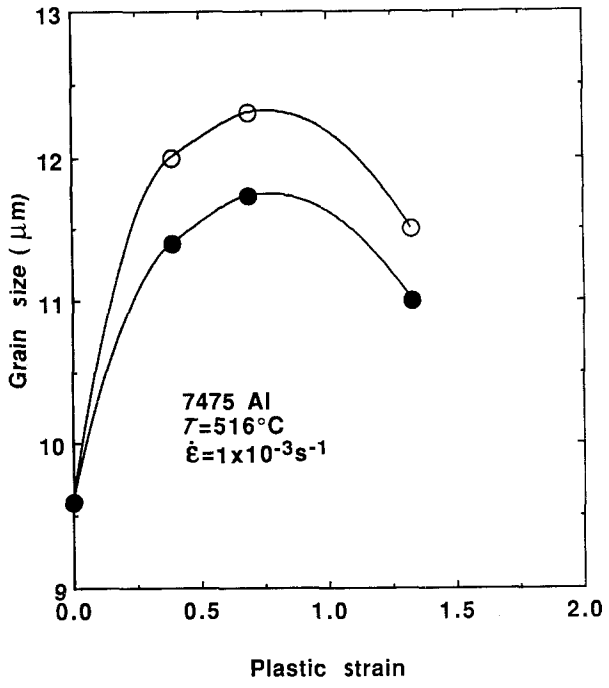

Figure 1 Effect of electric field on grain growth during superplastic deformation (true strain). E = ○, 0; ●, 2 kV cm^{-1}.

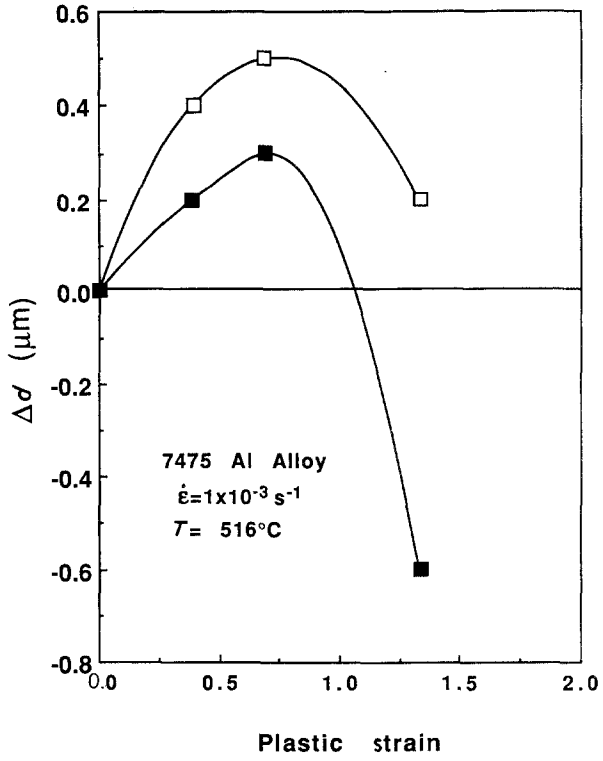

Figure 2 Increment of grain size due to superplastic flow against true plastic strain as a function of electric field. E = □, 0; ■, 2 kV cm^{-1}.

with strain is observed during superplastic deformation. However the present careful quantitative metallography revealed several interesting features concerning grain growth in this alloy. Fig. 1 shows that during superplastic deformation the grain size first increased with plastic strain and then decreased. Further, the electric field retarded grain growth at all plastic strains. However, Fig. 1 does not reflect the actual strain-induced grain growth behaviour, because the time at temperature increased with plastic strain. A better way to show the effect of strain on grain growth is by Fig. 2, where the difference in grain size between the deformed and undeformed (grip region) condition for the same heating time is plotted as the function of plastic strain. In this way the effect of different heating times is eliminated. Strain-enhanced grain growth at the smaller strains and a reduction in grain size at the higher plastic strains are now clearly identified, and also the retarding effect of the electric field.

The optical and TEM observations revealed that the reduced grain size at the larger strains was in part related to dynamic recrystallization which had occurred in the DFZ (see Fig. 3). The optical micrograph in Fig. 3a shows the grain structrure at the highest plastic strain $\varepsilon_p = 1.35$. Small grains are evident at some of the triple junctions of the larger grains. In some cases these small grains had a curved boundary on one side, and their morphology was similar to that of growing new grains. The TEM micrograph in Fig. 3b shows one of the many small grains which were observed. A curved and growing boundary is here clearly evident. However, most of the new grains had relatively straight boundaries, as in Fig. 3c. All of the newly formed grains were practically free of dispersoid particles and dislocations, indicating that they had formed in the DFZ. The above characteristics all suggest that these small grains result from dynamic recrystallization in the DFZ.

3.2. Dispersoid-free zone

Superplastic deformation led to the formation of DFZs adjacent to the grain boundaries. Optical microscope observations on the deformed state indicated that their width was larger with the electric field. However the width was difficult to measure for this microstructural state because of the low contrast between the DFZ and the matrix. Better contrast occurred for the precipitated state, giving the microstructure shown in Fig. 4. It was noted that the DFZs were widest at the grain-boundary segments which lay perpendicular to the extension (stressing) direction, and that their width increased with the electric field. The effect of the electric field on the mean width $\bar{S}$ in the extension direction and on the ratio of width to spacing $\bar{L}$ as a function of plastic strain is shown in Fig. 5. In addition to the increase in width of the DFZs with electric field, there occurred an increase in the size of the dispersoid particles in the grain matrix and in the vicinity of the DFZs (Fig. 6).

The TEM observations on the deformed state revealed that the DFZs were relatively free of dispersoid particles and dislocations (Fig. 7). Moreover, for the precipitated state they were free of precipitates, whereas extensive precipitation occurred in the adjacent grain interior (Fig. 8). It should be noted in Figs 7 and 8 that the dispersoids and precipitates delineate the DFZ boundaries. Although not clearly evident in these figures, in general the dispersoids were larger in the specimens deformed with the electric field. Also worthy of mention is that the Zn content of the DFZ was higher than in the grain interior, and that the electric field increased the difference [17].

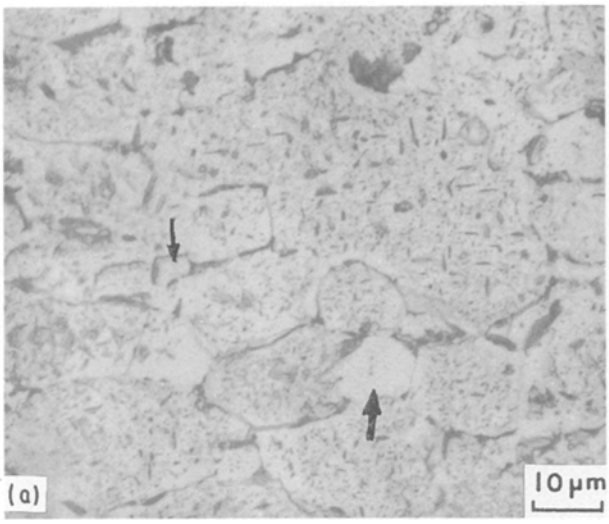

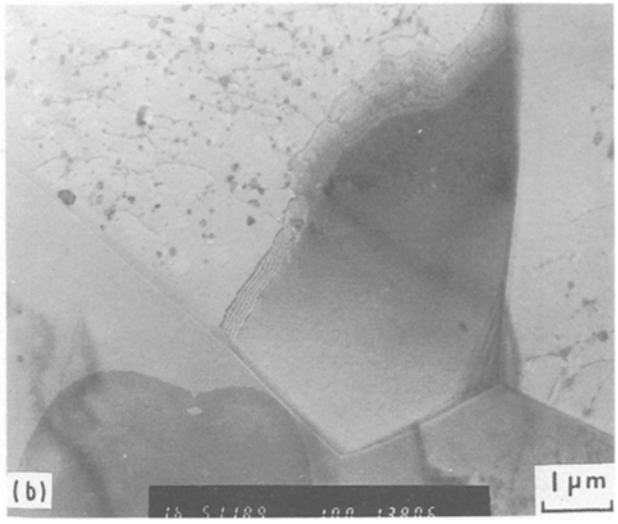

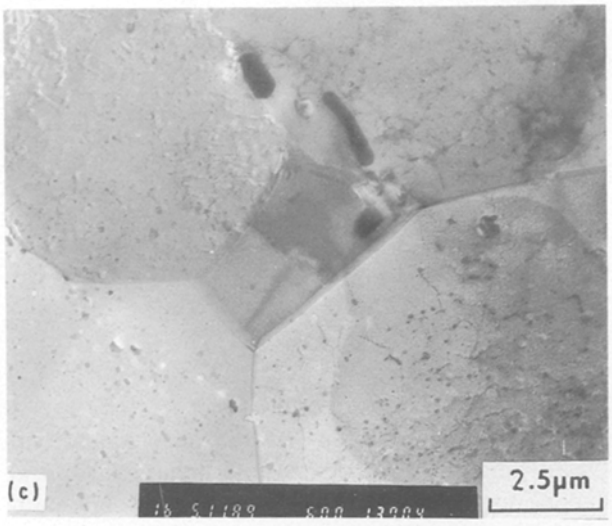

Figure 3 Evidence of dynamic recrystallization: (a) optical micrograph showing recrystallized grains; (b) and (c) TEM micrographs showing recrystallized grains in DFZ.

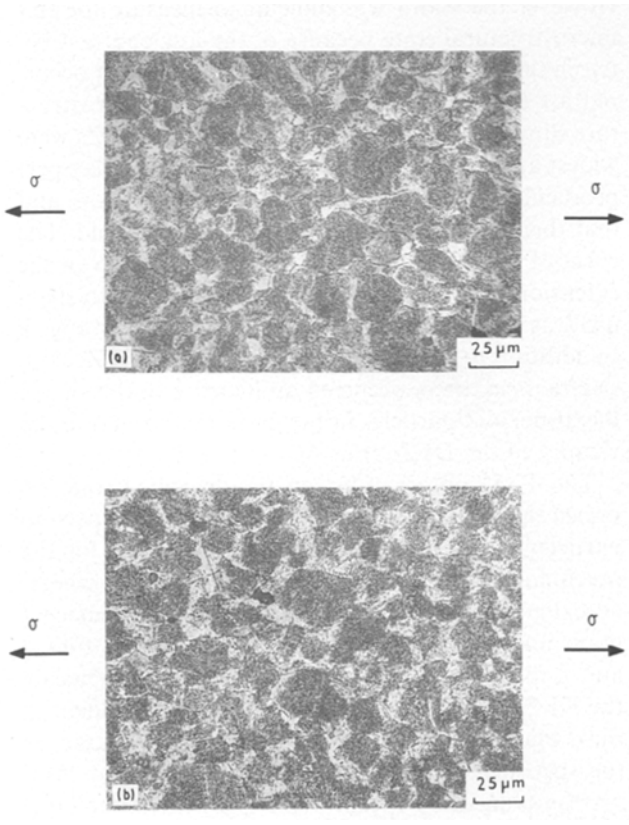

Figure 4 Optical micrographs of the precipitated state showing the DFZs at $\varepsilon_p = 0.7$: E = (a) 0; (b) 2 kV cm^{-1}.

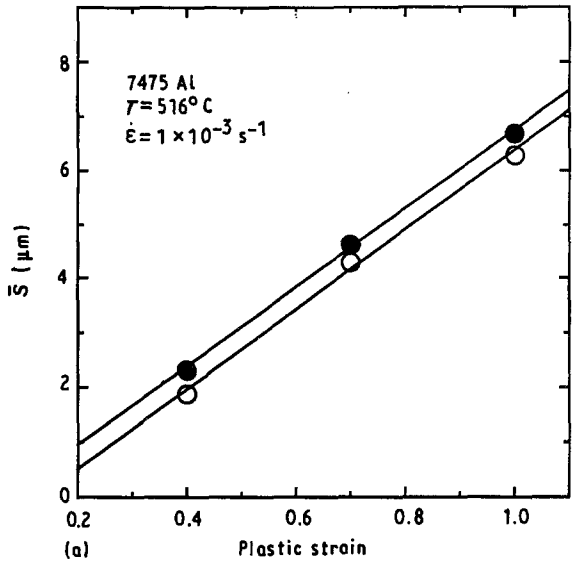

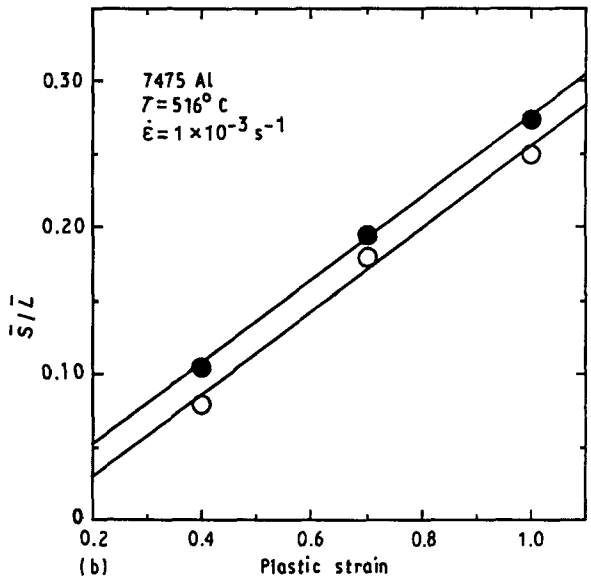

Figure 5 Effect of electric field on the DFZ size: (a) mean DFZ width $\bar{S}$ against plastic strain; (b) ratio of mean DFZ width $\bar{S}$ to mean DFZ spacing $\bar{L}$ against plastic strain. E = ○, 0; ●, 2 kV cm^{-1}.

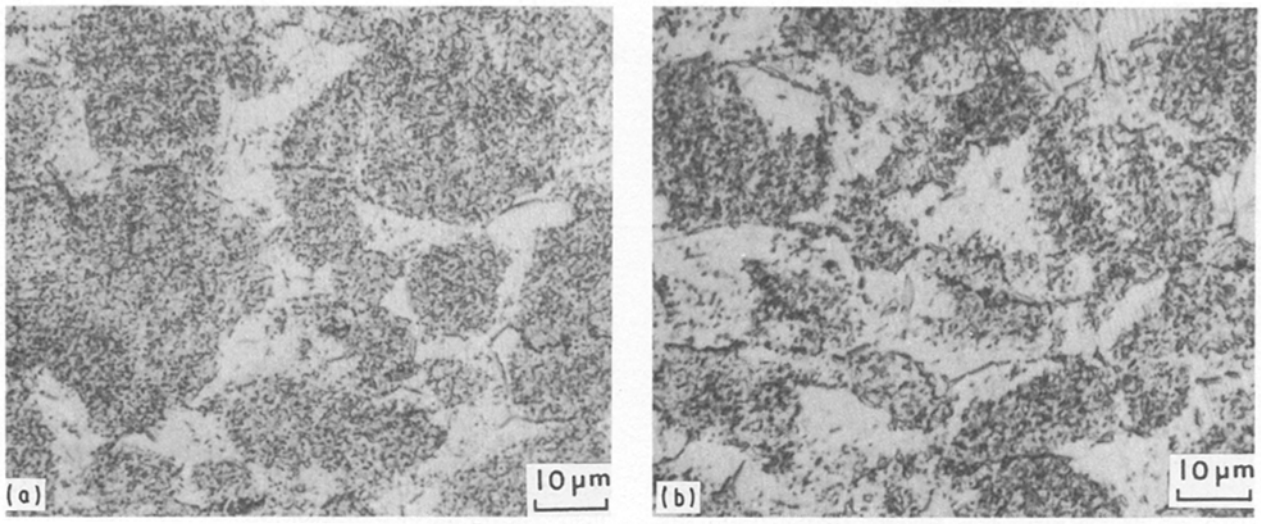

Figure 6 Higher-magnification optical micrographs of the precipitated state ($\varepsilon_p = 0.7$): E = (a) 0; (b) 2 kV cm^{-1}.

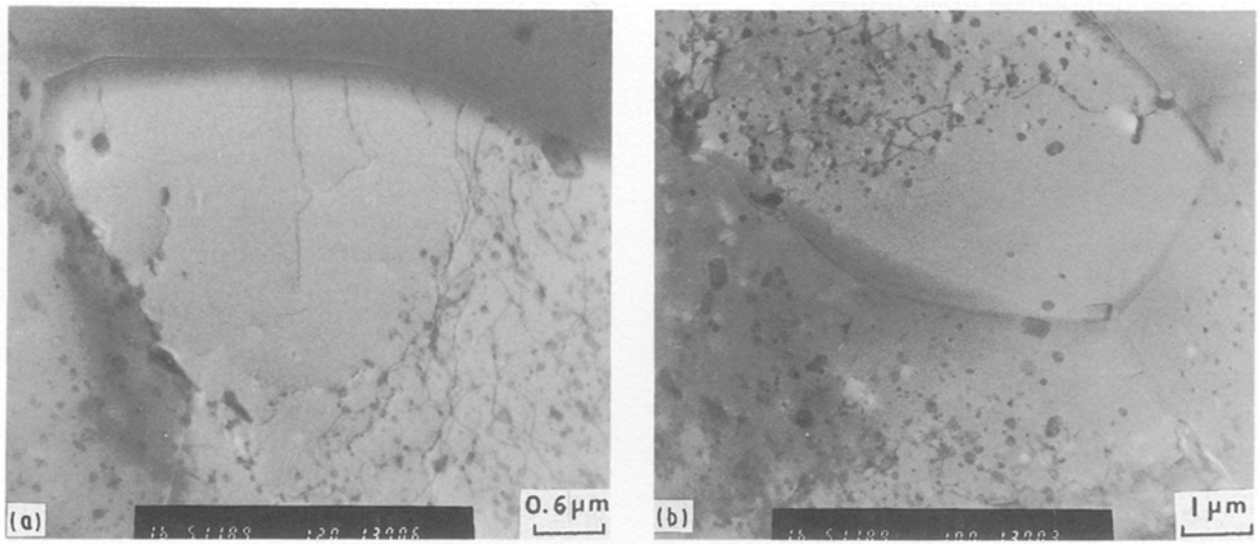

Figure 7 TEM micrographs of the deformed state ($\varepsilon_p = 0.7$): E = (a) 0; (b) 2 kV cm^{-1}.

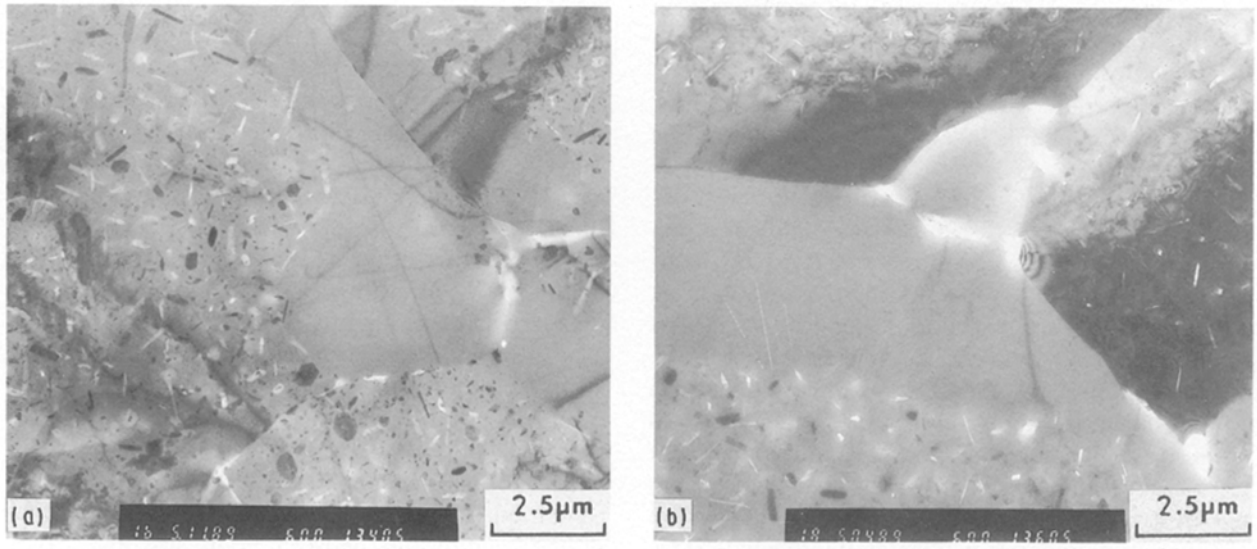

Figure 8 TEM micrographs of the precipitated state ($\varepsilon_p = 0.7$); E = (a) 0; (b) 2 kV cm^{-1}.

3.3. Grain interior

Figs 3, 4 and 6–8 also show the structure of the interior regions of the grains, which are surrounded by the DFZs. The prominent microstructural feature for the deformed state is the dispersoids, with some dislocations in their midst and pinned by them (Fig. 7). For the precipitated state, numerous needle-like particles occur along with the dispersoids (Fig. 8). Again, the size of the dispersoid particles was in general larger for the specimen deformed with the electric field (Fig. 6). An increase in the size of the dispersoids with electric field was also noted in sections taken from the grip regions of the test specimens, which had not been deformed but merely heated in the electric field. Also worthy of mention is that the dislocation density in the grain interior of specimens deformed with an electric field was smaller than without the field.

4. Discussion

4.1. Strain-modified grain growth

Strain-enhanced grain growth has been observed in many alloys, including the 7475 Al alloy. The earlier studies [12, 13, 18] have shown that the grain size increases with increasing plastic strain ε, and decreasing strain rate $\dot{\varepsilon}$. To describe this behaviour, Wilkinson and Caceres [18] suggested a relation of the form

$$\Delta d_\varepsilon = K_\varepsilon \varepsilon \dot{\varepsilon}^{-p} \tag{1}$$

where $p = 0.25$ over a certain range of test conditions, and Δd_ε is the strain-enhanced portion of the grain growth, i.e. the increment left after the grain growth produced by static annealing for the same time is subtracted. At intermediate strain rates (10^{-5} –$10^{-2}\,s^{-1}$) they proposed that [12]

$$\dot{d} = \lambda d_0 \dot{\varepsilon} \tag{2}$$

where $\lambda \cong 1$, $\dot{d}$ is the grain growth rate, and d_0 the initial grain size. According to Equation 2, a linear Δd_ε against ε relation should be observed in a constant extension rate test, whereas according to Equation 1 the grain size in a constant crosshead speed test should increase at a rate faster than given by a linear Δd_ε–ε relation, due to the concurrent decrease in plastic strain rate during extension. In contrast to these predictions, a slow-down in grain-growth rate with plastic strain was observed in the present study, and even a reduction in grain size occurred at the higher strain.

A reduction in grain size with strain has been observed by others [19, 20] in the 7475 alloy at strain rates of 10^{-3}–$10^{-2}\,s^{-1}$. Ghosh and Raj [19] interpreted this to result from dynamic recrystallization. Alternatively, Wert and Varloteaux [20] suggested that subgrain boundary formation may lead to the observed grain refinement. Dynamic recrystallization is more likely to be responsible for the reduction in grain size at the highest strain observed in the present tests, because most of the new grains which formed in the DFZ had large-angle boundaries. The formation of subgrain boundaries may be an intermediate stage of dynamic recrystallization. It thus appears that grain-boundary migration, which occurred concurrently with DFZ formation, was controlling at small strains leading to grain growth, but dynamic recrystallization of the DFZ dominated at the higher strains.

The reason for the retardation of grain growth by an electric field is not clear at this time. We offer the following speculations. The reduced grain growth at small strains may be the result of a reduction of grain boundary mobility *per se* by the electric field. However, there are two additional factors which play a role in grain-boundary migration during superplastic flow: namely, transgranular slip and grain boundary particles. Transgranular slip creates ledges on the grain boundaries and in turn promotes grain boundary migration. As seen in Fig. 7, less dislocation activity was observed in the specimens deformed with electric field. The diminished dislocation activity could lead to a reduced grain-boundary migration rate and less grain growth. Moreover, grain boundary dispersoids can retard grain-boundary migration by pinning the grain boundaries, which is believed to be the reason for the stable grain size of 7475 Al. Grain-growth rate is given by [21]

$$\dot{d} = MF(\Delta\mu) \tag{3}$$

where M is a constant related to mobility and F is the drag force which retards grain boundary migration, being a function of the $\Delta\mu$ (the chemical potential difference across a curved boundary). For materials containing fine dispersoid particles, the drag force is [22]

$$F = 3 f_v \gamma_b \Omega / r \tag{4}$$

where f_v and r are the volume fraction and average radius of the particles, respectively, γ_b is the boundary free energy, and Ω the atomic volume. It should be noted that f_v and r are those of the particles located at or near the grain boundaries. In the specimens with electric field, there was a higher volume fraction of grain-boundary dispersoids and their average size was larger. The higher f_v may, however, have overwhelmed the larger r in the specimens with field and thus be the dominant factor in retarding grain-boundary migration.

Another possible reason for the reduced grain size with the electric field is that more extensive dynamic recrystallization occurs with the field. Since dynamic recrystallization occurred in the DFZ, the larger area fraction of DFZ in the electric field will result in more extensive dynamic recrystallization, and in turn a smaller grain size.

A retardation of the strain-enhanced grain growth in the specimens with field is expected to have an influence on their superplastic deformation behaviour. The lower flow stress and work-hardening rate of specimens deformed in an electric field [14, 15, 17] could be partly due to their smaller grain size. Furthermore, the decreased grain growth in specimens with field may have contributed to the reduction in cavitation during the superplastic flow [16], in view of the relationship between grain size and cavity nucleation.

4.2. DFZ contribution to superplastic deformation

In 7475 Al, Wert and Varloteaux [20] observed DFZs at grain boundaries of all orientations to the specimen axis, whereas in the present study DFZs formed mainly at the boundaries normal to the extension direction. This suggests that grain-boundary diffusion creep may be an important mechanism for DFZ formation [10, 11, 23]. The diffusion creep strain ε_{DC} can be evaluated from the DFZ width according to [10, 11]

$$\varepsilon_{DC} = \bar{S}/\bar{L} \tag{5}$$

The plots in Fig. 5 thus give the diffusion creep strain without and with electric field. These data indicate that the contribution of diffusion creep strain to total strain ε_t increases slightly with plastic strain. This may be partly related to the decrease in strain rate with increasing plastic strain in our constant extension rate tests, because it has been shown that the ratio $\varepsilon_{DC}/\varepsilon_t$ increases with decreasing strain rate [23]. The magnitude of the ratio $\varepsilon_{DC}/\varepsilon_t$ in the present study is about 18% ($\varepsilon_p = 0.4$) to 26% ($\varepsilon_p = 0.9$) for specimens without field and 25% ($\varepsilon_p = 0.4$) to 29% ($\varepsilon_p = 0.9$) for the specimens with field. These values are similar to those reported for Zn–22Al [24] and Mg–0.5Zr [10] at about the equivalent deformation temperature of $0.8T_M$.

The electric field may have promoted the diffusion creep which occurs during superplastic deformation by accelerating vacancy diffusion along grain boundaries. The detailed mechanism by which this would occur is not clear, and further work is necessary. Accelerated diffusion creep in an electric field would have a significant influence on superplastic deformation behaviour. For example, the higher strain-rate sensitivity in specimens with electric field [14, 15, 17] could arise from a larger contribution of diffusion creep, which is Newtonian viscous and has a high strain-rate sensitivity. In addition, the lower cavitation in specimens with electric field [16] may have its origin in the effect of diffusion creep on the accommodation of grain boundary sliding. More complete accommodation due to increased diffusion creep would retard the nucleation of cavities and in turn reduce cavitation in specimens with an electric field.

It is of additional interest that precipitation did not occur in the DFZs for the slow cooling rate. This may have resulted from the lack of dislocations in the DFZs (which may be the nucleation sites for the precipitates) or perhaps to the lower Zn content of the DFZ.

4.3. Effect of electric field on dispersoids and precipitates

Two effects of the electric field on secondary phases were noted in the present study: (i) it promoted the coarsening of dispersoids, especially in the vicinity of the grain boundaries; and (ii) it increased the volume fraction of DFZs, thereby requiring a greater solution of dispersoids in these regions and the development of conditions whereby precipitates do not form here during slow cooling. The increased solution of dispersoids is in some accord with the results of Klypin [25–27], who reported that an electric field enhanced the dissolution rate of secondary phases in Al alloys, including an Al–Zn–Mg–Cu alloy. However, it is not clear how an external electric field can exert an influence over the volume of a metallic material. One possibility is that the electric field enhances the concentration of vacancies at the specimen surface, which then diffuse rapidly into the interior along the grain boundaries. An alternative suggestion is that of Klypin [25], who proposed that an uneven electron density between phases and at grain boundaries could lead to the penetration of an electric field into the volume.

5. Summary and conclusions

1. Strain-enhanced grain growth was observed at low strains during the superplastic deformation of 7475 Al, but a strain-promoted reduction in grain size occurred at high strains. The latter was attributed to dynamic recrystallization.

2. An external electric field retarded grain growth at both low and high strains, possibly by slowing grain boundary migration at low strains and by increasing dynamic recrystallization at high strains.

3. The electric field also promoted the dissolution and coalescence of dispersoids adjacent to the grain boundaries, leading to the formation of a wider dispersoid-free zone (DFZ) during superplastic deformation.

4. The wider DFZ which occurred with an electric field suggests that diffusion creep makes a greater contribution to the superplastic deformation of 7475 Al when an electric field is applied.

5. No precipitate occurred in the DFZs upon slow cooling from the superplastic deformation temperature, in contrast to the extensive precipitation within the adjacent grains.

6. The reason for the observed effects of the electric field is not clear.

6. Acknowledgements

This research was sponsored jointly by Alcoa Research Laboratories and the US Army Research Office under Grant Nos DAAL03-86-K-0015 and DAAL03-89-K-0115. The authors wish to express their appreciation for the interest and encouragement of Dr J. Staley of Alcoa, and Drs G. Mayer, I. Ahmad and E. Chen of ARO.

References

1. J. W. EDINGTON, K. N. MELTON and C. P. CULTER, *Prog. Mater. Sci.* **21** (1976) 61.
2. J. W. EDINGTON, *Metal. Trans.* **13A** (1982), 703.
3. R. PEARCE, "Superplasticity – An Overview", (AGARD (NATO), Cranfield Institute of Technology, England, 1987) p. 1–1.
4. O. A. RUANO and O. D. SHERBY, *Mater. Sci. Engng* **56** (1982) 167.
5. C. H. CACERES and D. S. WILKINSON, *Acta Metall.* **32** (1984) 415.

6. M. SUREY, *Scripta Metall.* **18** (1984) 333.
7. J. PILLING and N. RIDLEY, in Proceedings of ICSMA (International Conference on Strength of Metals and Alloys) 7, Vol. 2, edited by H. J. McQueen, J.-P. Bailon, J. I. Dickson, J. J. Jones and M. G. Akben (Pergamon, Oxford, 1985) p. 823.
8. A. K. GHOSH: in "Deformation of Polycrystals: Mechanisms and Microstructure", edited by M. Hansen, A. Hordenell, T. Leffers and H. Lilholt (Risø National Laboratory, Denmark, 1981) p. 277.
9. R. I. KUZNETSOVA and O. A. KAIBYSHEV, *Sov. Phys. Dokl.* **26** (1981) 429.
10. ANWAR-VL KARIM, D. L. HOLT and W. A. BACKOFEN, *Trans. AIME* **245** (1969) 2421.
11. R. Z. VALIEV and O. A. KAIBYSHEV, *Acta Metall.* **12** (1983) 2121.
12. D. S. WILKINSON and C. H. CACERES, *J. Mater. Sci. Lett.* **3** (1984) 395.
13. R. ARROWOOD and A. K. MUKHERJEE, *Scripta Metall.* **18** (1984) 249.
14. H. CONRAD, W. D. CAO, X. P. LU and A. F. SPRECHER, *Scripta Metall.* **23** (1989) 697.
15. W. D. CAO, X. P. LU, A. F. SPRECHER and HANS CONRAD, *Mater. Sci. Engng.* **A129** (1990) 157.
16. H. CONRAD, W. D. CAO, X. P. LU and A. F. SPRECHER, *Mater. Sci. Engng.*, **A138** (1991) 247.
17. W. D. CAO, X. P. LU, A. F. SPRECHER and HANS CONRAD, "Superplasticity in Aerospace II", edited by T. L. McNelley and H. C. Heikkenan (TMS–AIME, Warrendale, PA, 1990) p. 269.
18. D. S. WILKINSON and C. H. CACERES, *Acta Metall.* **32** (1984) 1335.
19. A. K. GHOSH and R. RAJ, in "Superplasticity", edited by B. Baudelet and M. Surey (Editions du CNRS, Paris, 1985) p. 11.1.
20. J. A. WERT and A. VARLOTEAUX, in "Aluminum Alloys: Their Physical and Mechanical Properties" Vol. II, edited by E. A. Starke and T. H. Sanders (EMAS, Warley, UK 1986) p. 1255.
21. J. D. VERHOEVEN, "Fundamentals of Physical Metallurgy" (Wiley, New York, 1975) p. 201.
22. J. W. MARTIN and R. D. DOCHERTY, in "Stability of Microstructures" (Cambridge University Press, Cambridge, 1976) p. 234.
23. T. B. GIBBOW, *Metal. Sci.* **6** (1972) 13.
24. I. I. NOVIKOV, V. K. PORTNOY and T. E. TERENTIEVA, *Acta Metall.* **25** (1977) 1139.
25. A. A. KLYPIN, *Metalloved Term. Obrab. Met.* No. 3 (1979) 12.
26. *Idem, Izv. V.U.Z., Tsvet. Metall.* No. 4 (1978) 101.
27. *Idem, Light Metal Age* No. 12 (1979) 18.

Received 19 March
and accepted 9 July 1991